Arbitrary UWB Pulse Generation and Optimum Matched-Filter Reception

I. Arnedo, I. Arregui, M. Chudzik, A. Lujambio, M. A. G. Laso, T. Lopetegi
Dept. of Electrical & Electronic Engineering
Public University of Navarre
Pamplona, Navarre, Spain
israel.arnedo@unavarra.es

Joshua D. Schwartz, José Azaña
Énergie, Matériaux et Télécommunications
Institut National de la Recherché Scientifique – (INRS-ÉMT)
Montreal, Quebec, Canada

David V. Plant
Dept. of Electrical and Computer Engineering
McGill University
Montreal, Quebec, Canada

***Abstract*—This paper explores a general synthesis technique previously developed by the authors for designing microwave devices with fully customized temporal/spectral responses and its application in the context of Ultra-Wide Band (UWB) communications. The theoretical foundations of the exact analytical series solution for the synthesis problem are first discussed. The proposed synthesis technique enables the realization of arbitrary filter responses limited only by causality, passivity and stability. A simple and efficient implementation of the synthesis algorithm is also presented. Finally, we demonstrate the application of the microwave synthesis technique for UWB applications: key components for the generation and optimal reception of Impulse-Radio UWB signals are designed and demonstrated. In particular, an UWB pulse-shaper and a matched-filter are experimentally demonstrated in conventional microstrip technology.**

Keywords- Ultra-Wide Band technology; matched-filter; arbitrary pulse generation; pulse-shaper; microstrip technology;

I. INTRODUCTION

The Federal Communications Commission (FCC) impelled research into Ultra-Wideband (UWB) systems by granting unlicensed use of the 3.1 to 10.6 GHz frequency band, as well as other bands, for signals with spectral power density below -41.2dBm/MHz [1]. Application areas that have been targeted for UWB technology include high data-rate wireless communication [2], [3], homeland security [4], and specialized radar imaging [5].

Many of these applications require pulses with tailored shapes [6], [7]. Several techniques for generating customized UWB pulse waveforms have been proposed in both CMOS technology [8] and using photonics components [9]. CMOS solutions are limited in regards to the temporal shapes that can be practically synthesized [8] and optical hardware tends to be costly and difficult to integrate with microwave technologies [9]. The optimum reception of such pulses can be accomplished by means of matched-filters that can be understood as passive correlators [10]-[12].

We have recently reported a general synthesis method [13], enabling the design of waveguides and transmission lines with nearly any target impulse response. In planar technology, this method leads to structures that can be seen as a generalization of the Electromagnetic Bandgap (EBG) structures proposed for the first time by T. Itoh in the late 90's [14] drawing a renewed attention to the periodic structures and shedding new light on this classic field. Although originally implemented by drilling a periodic array of holes in the dielectric of a planar microwave transmission line, better performance and easier fabrication were shown to be possible by simply etching a sinusoidal perturbation directly into the microstrip ground plane [15]. Apodization techniques were reported to reduce the ripple in the stopband of the EBG structure, while chirping techniques were used to increase the rejected bandwidth [16].

The coupled-mode theory has been successfully employed to model these structures, assuming single-mode operation, providing a valuable physical insight into the operation of the devices and a didactic link with the well established topic of Bragg Gratings in the optical regime [17]. Further research based on the coupled-mode theory lead to a synthesis technique for building a reflection-mode transmission line or waveguide with any target causal, passive and stable frequency response [13]. This technique contains two steps. In the first step, the necessary coupling coefficient as a function of distance along the line or waveguide is obtained from the target frequency response. Then, the coupling coefficient is used to determine the necessary physical dimensions at each point along the propagation axis, giving rise to structures with smooth profile.

In this paper, an efficient computer implementation of the aforementioned synthesis technique is proposed. Based on this method, we develop a simple procedure for re-shaping an input stimulus such as an impulse into any desired UWB pulse waveform. The flexibility offered by the synthesis method is further demonstrated by designing the matched-filtering device adapted to a given arbitrary signal [18], [13]. The proposed applications are illustrated by experimentally demonstrating, with simple microstrip circuits, a pulse shaper aimed to the generation of UWB impulses complying with the FCC mask as well as a matched-filter also intended for Impulse-Radio UWB.

II. EXACT SYNTHESIS

Starting from the simplified system of coupled-mode equations that model a waveguide, assuming single-mode operation [17], our aim is to synthesize a physical device with a

This work was supported by the Spanish Government under the project TEC2008-06871-C02-01 and by the Natural Sciences and Engineering Research Council of Canada (NSERC) through a Strategic Project Grant. I. Arnedo has developed part of this work at the INRS-ÉMT

prescribed arbitrary causal, stable and passive frequency response. Let the coupled-mode equations system be:

$$\begin{aligned} \frac{da^+}{dz} &= -j\cdot\beta\cdot a^+ + K\cdot a^- \\ \frac{da^-}{dz} &= j\cdot\beta\cdot a^- + K\cdot a^+ \end{aligned} \tag{1}$$

where $\hat{\vec{E}} = a^+\cdot\vec{E}^+ + a^-\cdot\vec{E}^-$ and $\hat{\vec{H}} = a^+\cdot\vec{H}^+ + a^-\cdot\vec{H}^-$ are the total electric and magnetic fields present in the waveguide, $\vec{E}^+$, $\vec{E}^-$, $\vec{H}^+$ and $\vec{H}^-$ being the (*x,y*) dependent part of the electric and magnetic fields for the forward (+) and backward (–) traveling waves, and *z* being the propagation axis. In (1), *K* is the coupling coefficient between the forward and backward traveling waves and β is the propagation constant.

Taking advantage of the fact that *K*(*z*) in our system is a real function and hence *K*(*z*) = K^*(*z*), where * stands for complex conjugate, we can rearrange the equations system (1) in order to express it in the form of the Zakharov-Shabat system of quantum mechanics [19]:

$$j\cdot\begin{pmatrix} \frac{d}{dz} & -K \\ K^* & \frac{-d}{dz} \end{pmatrix}\cdot\begin{pmatrix} a^+ \\ a^- \end{pmatrix} = \beta\cdot\begin{pmatrix} a^+ \\ a^- \end{pmatrix} \tag{2}$$

To solve (2), we assume that the coupling region starts at *z* = 0 and therefore:

$$K(z) = 0 \quad , \quad z < 0 \tag{3}$$

From this condition, causality restrictions will be derived and applied after reformulating the problem in the inverse Fourier Transform domain (τ domain). It is worth noting that the variable τ, measured in length units, is related with the time variable through the phase velocity, v_p, i.e. $\tau = v_p\cdot t$, assuming that the phase velocity remains constant with frequency. Applying properties of the solutions of the Zakharov-Shabat system, the following set of Gel'fand-Levitan-Marchenko (GLM) coupled integral equations can be obtained [13]:

$$\begin{aligned} &A_1(z,\tau) + \int_{-\tau}^{z} A_2^*(z,y)\cdot F(y+\tau)\cdot dy = 0 \quad , \quad |z| > \tau \\ &A_2(z,\tau) + F(z+\tau) + \int_{-\tau}^{z} A_1^*(z,y)\cdot F(y+\tau)\cdot dy = 0, \ |z| > \tau \end{aligned} \tag{4}$$

where $A_{1,2}(z,\tau)$ are auxiliary functions and $F(\tau)$ is the inverse Fourier Transform of the desired S_{11}-parameter:

$$F(\tau) = \frac{1}{2\pi}\int_{-\infty}^{\infty} S_{11}(\beta)\cdot e^{j\cdot\beta\cdot\tau}\cdot d\beta \tag{5}$$

We must stress that in order to formulate the problem in the τ-domain using the Fourier transformation, we assume that propagation constant β is constant with *z*.

Finally, *K*(*z*) can be deduced from the auxiliary functions in the GLM system. Employing again the inverse Fourier Transform, using (1) and (4), assuming that *K* is constant with β, and applying causality considerations, the following equation can be inferred [13], [19]:

$$K(z) = -2\cdot F(2z) - 2\cdot\int_{-z}^{z} A_1^*(z,y)\cdot F(y+z)\cdot dy \tag{6}$$

If the integral term of (6) is neglected, the zero-order approximation for the coupling coefficient $K(z) \approx -2\cdot F(2z)$ is obtained. The final step is to solve the GLM system by using an iterative method. Reorganizing (4) yields:

$$\hat{A}_1(z,\tau) = -\int_{-\tau}^{z} \hat{A}_2^*(z,y)\cdot F(y+\tau)\cdot dy \tag{7a}$$

$$\hat{A}_2(z,\tau) = -F(z+\tau) - \int_{-\tau}^{z} \hat{A}_1^*(z,y)\cdot F(y+\tau)\cdot dy \tag{7b}$$

Neglecting the integral term in (7b), this equation can be written as:

$$\hat{A}_2(z,\tau) \cong -F(z+\tau) \tag{8}$$

Introducing (8) into (7a) we obtain:

$$\hat{A}_1(z,\tau) \cong \int_{-\tau}^{z} F^*(z+x_1)\cdot F(x_1+\tau)\cdot dx_1 \tag{9}$$

Introducing (9) into (6), the first-order approximation for the coupled coefficient is obtained:

$$K(z) = -2F(2z) - 2\int_{-z}^{z} dx_1 F(x_1+z)\int_{-x_1}^{z} dx_2 F(z+x_2)F^*(x_1+x_2)$$

Therefore, if we proceed in an iterative manner introducing (9) in (7b) and then the result of this operation in (7a) to update (6), taking also into account that $F(\tau)$ will be real for a physical device, we arrive at the exact analytical series solution for the coupling coefficient given in (10) below, where $x_i' = x_i + x_{i-1} - 2z$ for $i > 1$.

The pseudocode of an efficient computer algorithm to solve this iterative process is now presented. In this algorithm, the exact infinite analytical series solution given in (10) is truncated and an approximation of the coupling coefficient

$$K(z) = -2F(2z) - 2\int_0^{2z} dx_1 F(x_1) \int_0^{x_1} dx_2' F(x_2') F(x_2' - x_1 + 2z) - 2\int_0^{2z} dx_1 F(x_1) \int_0^{x_1} dx_2' F(x_2') \int_0^{x_2} dx_3' F(x_3') \int_0^{x_3} dx_4' F(x_4') F(x_4' - x_3 + 2z)$$
$$- \cdots - 2\int_0^{2z} dx_1 F(x_1) \int_0^{x_1} dx_2' F(x_2') \int_0^{x_2} \cdots \int_0^{x_{2N-1}} dx_{2N}' F(x_{2N}') F(x_{2N}' - x_{2N-1} + 2z) - \ldots - \quad (10)$$

is calculated. Firstly, the order of the approximation, *NGLM*, is chosen. The accuracy of the method will depend on the number of terms taken from the series solution, which equals *NGLM* + 1. The input function $S_{11}(\beta)$, $\forall \beta \in [0, \beta_{\max}]$, contains the user specifications for the target frequency filtering response. The value of $F(\tau)$ can be rapidly calculated with the aid of an inverse Fast Fourier Transform (iFFT) following (5). The integrals in (10) can be solved efficiently in a recursive manner, since they are related according to the following equation:

$$I_i(x_i) = \int_0^{x_i} dx_{i+1} \cdot F(x_{i+1}) \cdot I_{i+1}(x_{i+1} - x_i + 2z)$$

Thus, the pseudocode allowing for the calculation of *K*(*z*) from the target $S_{11}(\beta)$ can be very compact and efficient:

```
Input:   S11(β), ∀β ∈ [0, βmax]  or  F(τ), ∀τ ∈ [0, 2L]
         NGLM ≡ Order of the approximation

Output:  KGLM ≡ K(z)

F(τ) = iFFT(S11(β)) , ∀τ ∈ [0, 2L]
For zn ∈ [0, L]
{   V = F
    KGLMn = F(2zn)
    For i = 0  to  2·(NGLM − 1)
    {   U(u) = ∫0^u dt·F(t)·V(t − u + 2zn) ,  ∀u ∈ [0, 2L]
        V = U
        If i is even
        {   KGLMn = KGLMn + ∫0^2zn dt·F(t)·U(t)
        }
    }
    KGLMn = 2·KGLMn
}
```

Finally, it is important to stress that due to the fact that $K(z_i)$ is independent of $K(z_j)$, $\forall i \neq j$, the algorithm proposed here has good characteristics for parallel or distributed computation, which is an interesting feature for those situations where integrals need higher time to be computed.

III. UWB Applications

The series solution of the synthesis problem, implemented as in Section II, allows one to calculate the required coupling coefficient for a device featuring an arbitrary target frequency response. The arbitrary target response of the circuit can be defined in the time domain or, equivalently, in the frequency domain, being only limited by causality, passivity and stability. In this section, the synthesis method described above will be verified by designing and experimentally demonstrating an arbitrary pulse-shaper for UWB applications and a matched-filter also intended for Impulse-Radio UWB [2], [20], [12]. Both devices will be implemented in conventional microstrip technologies.

The expressions that relate the physical dimensions of the device and the coupling coefficient, calculated as explained above, depend on the technology used [13]. For the case of transmission lines, the coupling coefficient can be obtained from the characteristic impedance parameter, Z_0 [17]:

$$K = -\frac{1}{2} \cdot \frac{1}{Z_0} \cdot \frac{dZ_0}{dz} \quad (11)$$

As explained in [17], (11) assumes that Z_0 characterizes completely the propagation of the mode along the waveguide in terms of reflection. Under this assumption, we can solve (11) in order to obtain a close expression for the characteristic impedance as a function of distance:

$$Z_0(z) = Z_0(0) \cdot e^{-2 \cdot \int_0^z K(x) dx} \quad (12)$$

where $Z_0(0)$ is the characteristic impedance of the input port. The physical dimensions for microstrip technology are calculated from the characteristic impedance using classical expressions [21].

A. Design of UWB Pulse-Shapers

We approach UWB pulse synthesis by assuming some practical impulse generator creating impulses with spectrum $G(f)$. Our aim is the design of a pulse-shaping device of frequency response $H(f)$, see Fig. 1, for UWB signal generation. Some application-dependent auxiliary devices (e.g. antennas, directional couplers, power dividers, etc.) with responses $A(f)$ and $B(f)$ known *a priori* may be also present in the design [18]. Let $x(t)$ [$X(f)$] and $y(t)$ [$Y(f)$] be the input excitation and the desired UWB output response in time [frequency], respectively.

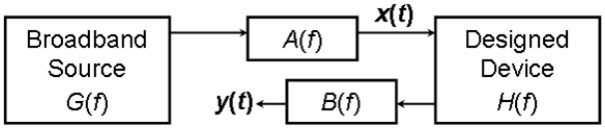

Figure 1. General schematic of the UWB pulse-shaper demonstration.

We can obtain the frequency response of the waveguide to be synthesized, $H(f)$, from the desired UWB output response, $Y(f)$, as:

$$H(f) = \frac{Y(f)}{X(f) \cdot B(f)} \cdot e^{-j \cdot 2 \cdot \pi \cdot f \cdot \tau_d} \tag{13}$$

where a linear phase term has been added to ensure causality (i.e., τ_d is some arbitrary delay).

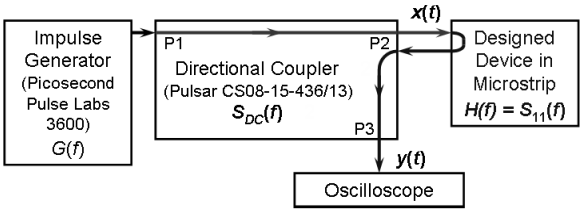

Figure 2. Experimental setup.

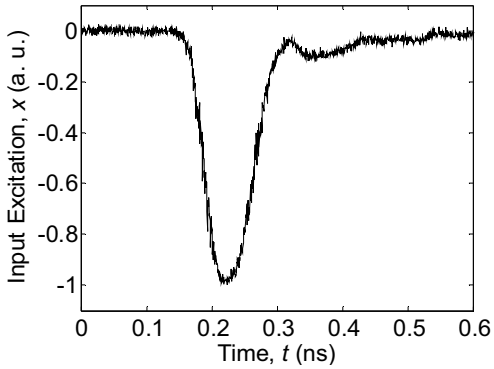

Figure 3. Input excitation, $x(t)$.

The experimental setup shown in Fig. 2 is used in our case to generate arbitrary UWB pulses in microstrip technology. A commercial impulse generator (Picosecond Pulse Labs 3600) transmitting through a commercial directional coupler (Pulsar CS08-15-436/13) generate the input excitation, $x(t)$, which is shown in Fig. 3 as measured with a sampling oscilloscope. The excitation signal is launched into the designed microstrip circuit, and the reflected signal from this device is routed to the oscilloscope through the other branch of the commercial directional coupler. According to (13), the target UWB pulse $y(t)$ is obtained if the designed device satisfies:

$$S_{11}(f) = \frac{Y(f)}{X(f) \cdot S_{DC32}(f)} \cdot e^{-j \cdot 2 \cdot \pi \cdot f \cdot \tau_d} \tag{14}$$

In this example, we seek to generate the fourth derivative of a Gaussian monocycle [6], whose expression is given in (15), with T_c = 0.25 ns and T_{au} = 0.102 ns, complying with the FCC mask:

$$y(t) = \frac{d^4}{dt^4}\left(A \cdot \frac{t - T_c}{T_{au}} \cdot e^{-2\left(\frac{t-T_c}{T_{au}}\right)^2} \right) \tag{15}$$

The necessary coupling coefficient of the pulse-shaper has been calculated introducing (14) and choosing $NGLM$ = 6 in the computer algorithm proposed at the end of Section II. The result is plotted in Fig. 4. The required characteristic impedance as a function of the propagation axis along the device is calculated through (12) and shown in Fig. 5.

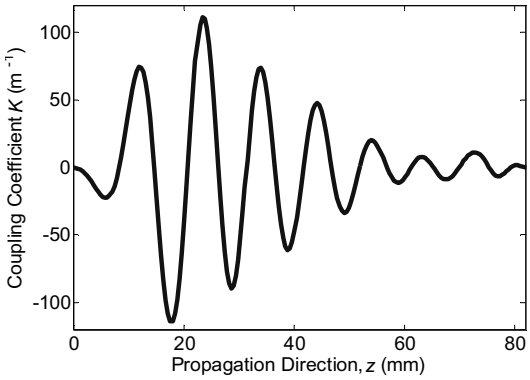

Figure 4. Coupling coefficient of the designed UWB microstrip pulse-shaper circuit.

We fabricated the microstrip circuit, see photograph in Fig. 6, to match this characteristic impedance profile by continuously varying the conductor strip-width according to classical microstrip design formulas [21]. The substrate employed was a RT/DUROID 5880 (thickness h = 0.508 mm, relative dielectric constant ε_r = 2.2) having 50-Ω impedance at the ports.

The target pulse is presented in both theory (thin line) and measurement (thick line) in the time-domain using a Tektronix CSA 8000 oscilloscope (see Fig. 7), and in the frequency domain (see Fig. 8) using a numerical Fourier Transform of the measured signal after employing time-gating to remove spurious reflections. Excellent agreement is observed between the target pulse shape and spectrum, and those corresponding to the measured results, which, moreover, clearly satisfy the prescribed UWB FCC mask.

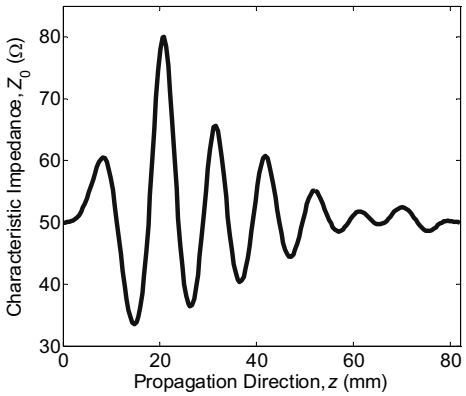

Figure 5. Characteristic impedance of the designed UWB microstrip pulse-shaper circuit.

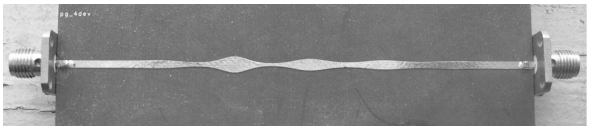

Figure 6. Photograph of the fabricated of the designed UWB microstrip pulse-shaper circuit.

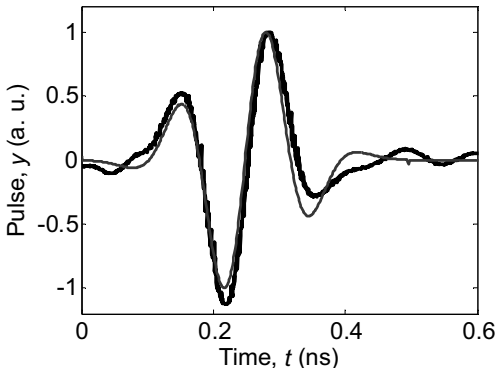

Figure 7. Fourth-derivative of a Gaussian monocycle: target signal (thin line), and measurement (thick line).

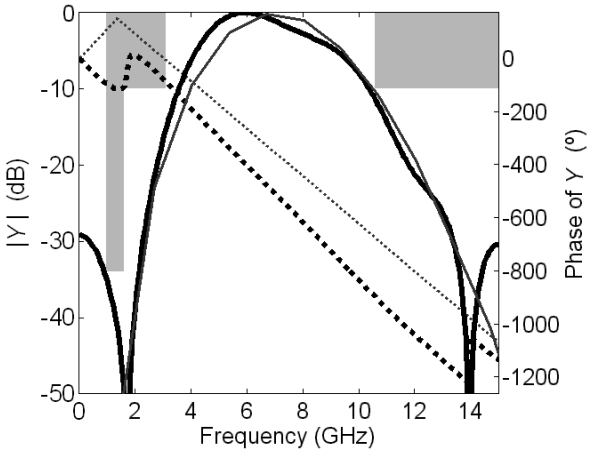

Figure 8. Magnitude (solid line), and phase (dotted line) of the spectrum of the target pulse (thin line), and of the Fourier Transform of the measured pulse (thick line). The shaded area represents the FCC UWB mask.

B. Synthesis of Matched-Filters

As is well known [10], a filter matched to a signal $s(t)$ has an impulse response:

$$F(t) = s(t_d - t) \tag{16}$$

where t_d is the time delay between the signal arrival and the output peak where the signal-to-noise ratio is maximized [12]. Moreover, it has been reported that when very short pulses are used [18], [9], it is challenging to design a matched-filter for optimum detection [11].

In the next example, the signal to be detected, $s(t)$, is an UWB sinusoidal burst that satisfies:

$$s(t) = A \cdot \sin(2\pi \cdot f_0 \cdot t) \cdot [\cos(\pi \cdot f_0 \cdot t)]^2 . \tag{17}$$

where f_0 = 2.5 GHz. The fractional bandwidth (at -10 dB) of the signal is around 120%. This particular signal does not comply with the FCC-specified mask, but is intended only as a proof of concept.

The impulse response of the matched-filter, $F(t)$, is obtained by introducing (17) into (16) and is shown in Fig. 9 (thin solid line). We employ $F(t)$ along with a 6th-order approximation (*NGLM* = 6) in the proposed computer algorithm of section II in order to obtain the necessary coupling coefficient, which is plotted in Fig. 10. Its corresponding characteristic impedance profile has been obtained from (12) and is shown in Fig. 11. The resulting filter layout is depicted in Fig. 12 (a *Rogers RO3010*™ substrate has been used with thickness h = 1.27 mm, relative dielectric constant ε_r = 10.2, and 50 Ω impedance ports). The filter was measured with an *Agilent*™ 8722 Vector Network Analyzer. The impulse response of the filter, obtained as the inverse Fourier Transform of the measured S_{11}-parameter, is shown also in Fig. 9 (thick solid line). Finally, Fig. 13 shows the target (thin solid line) and measured (thick solid line) S_{11}-parameter of the matched-filter.

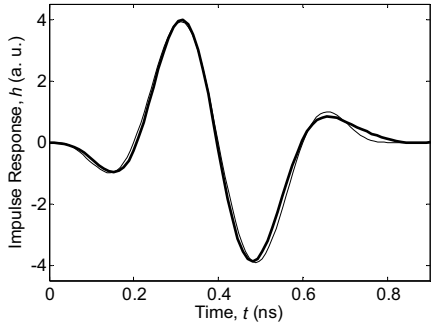

Figure 9. Target impulse response (thin solid line) and inverse Fourier Transform of the measured S_{11}-parameter (thick solid line) of the synthesized matched-filter.

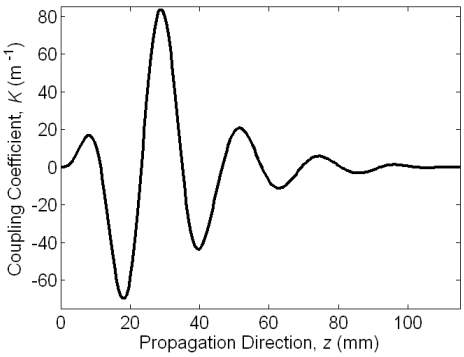

Figure 10. Coupling coefficient of the synthesized matched-filter.

The excellent agreement between the target and the measured responses for both the pulse-shaper and the matched-filter confirms the accuracy of the proposed synthesis method. The slight differences found can be attributed to the assumptions made in the synthesis method (e.g. the phase constant for a given frequency does not vary along the device length and the coupling coefficient does not vary with frequency), which are not fully satisfied in microstrip technology. In addition, the losses of the experimental device

and fabrication tolerances were not considered in the design procedure.

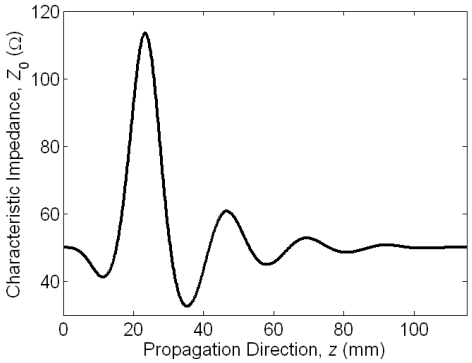

Figure 11. Characteristic impedance of the synthesized matched-filter.

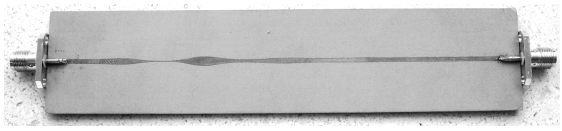

Figure 12. Photograph of the fabricated matched-filter.

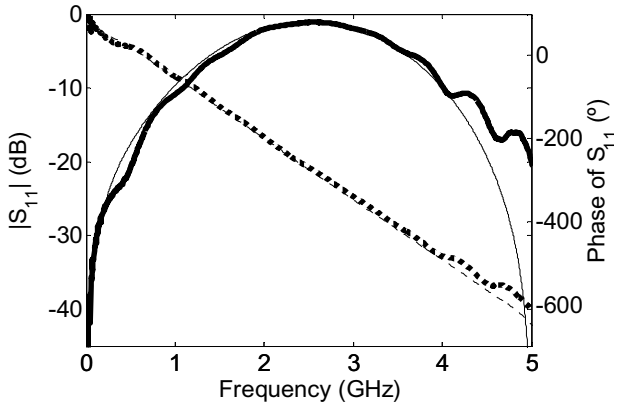

Figure 13. Magnitude (solid line), and phase (dotted line) of the frequency response of the synthesized matched-filter. The target (thin line), and measured (thick line) S_{11} parameters are given.

IV. Conclusion

We have developed a general and efficient algorithm that implements the exact analytical series solution for the synthesis problem of microwave filtering devices. This synthesis method enables the realization of a arbitrary filtering response, constrained only by causality, passivity and stability, and not necessarily limited to rational spectral transfer functions.

Two different device implementations of interest in UWB communication systems have been demonstrated in microstrip technology using our general synthesis technique, confirming its accuracy and usefulness in the UWB context. In particular, we have demonstrated a passive and readily integrable microwave solution for arbitrarily re-shaping a given temporal impulse into any desired UWB pulse waveform. Secondly, a means to design the matched-filter of a UWB detection system has been successfully tested. Our general design technique can also be used taking into account any other additional elements required in the transmitting or receiving subsystems, provided their frequency responses are known *a priori*. This may include a model of the channel, which could help minimize the distortion of the received pulse.

References

[1] Federal Communications Commission (FCC), (2006, August), *Part 15 Rules for Unlicensed RF Devices* [Online] Available: http://www.fcc.gov/oet/info/rules.

[2] R. J. Fontana, "Recent System Applications of Short-Pulse Ultra-Wideband (UWB) Technology," *IEEE Trans. Microw. Theory Tech.*, vol. 52, no. 9, pp. 2087-2104, Sept. 2004.

[3] G. R. Aiello and G. D. Rogerson, "Ultra-Wideband Wireless Systems," *IEEE Microw. Magazine*, vol. 4, no. 2, pp. 36-47, June 2003.

[4] P. Withington, H. Fluhler, and S. Nag, "Enhancing Homeland Security with Advanced UWB Sensors," *IEEE Microw. Mag.*, vol. 4, no. 3, pp. 51-58, Sept. 2003.

[5] A.G. Yarovoy, L.P. Ligthart, J. Matuzas, and B. Levitas, "UWB Radar for Human Being Detection," *IEEE Aerospace and Electron. Sys. Magazine*, vol. 21, no. 3, pp. 10-14, March 2006.

[6] X. Chen, S. Kiaei, "Monocycle shapes for ultra wideband system," *IEEE Int. Symp. on Circuits and Systems,* vol. 1, pp. 597-600, May 2002.

[7] B. Allen, S. A. Ghorashi, and M. Ghavarm, "A review of pulse design for impulse radio," *IEE Seminar on Ultra Wideband Comm. Tech. and System Design*, pp. 93- 97, July 2004.

[8] Y. Bachelet, S. Bourdel, J. Gaubert, G. Bas, and H. Chalopin, "Fully Integrated CMOS UWB pulse generator," *Electronics Lett.*, vol. 42, no. 22, pp. 1277-1278, Oct. 2006.

[9] T. Kawanishi, T. Sakamoto, and M. Izutsu, "Ultra-Wide-Band Radio Signal Generation Using Optical Frequency-Shift-Keying Technique," *IEEE Microw. Wireless Compon. Lett.*, vol. 15, no. 3, pp. 153-155, Mar. 2005.

[10] G. L. Turin, "An introduction to matched filters," *IRE Transactions on Information Theory*, vol. 6, no. 3, pp. 311-329, Jun. 1960.

[11] H. L. Van Trees, *Detection, Estimation, and Modulation Theory*, New York: Wiley, 2001, pt. 1, ch. 4.4.1.

[12] A. B. Carlson, *Communication Systems*, Third Edition, New York, NY: McGraw-Hill Electrical and Electronic Engineering Series, 1986.

[13] I. Arnedo, M. A. G. Laso, F. Falcone, D. Benito and T. Lopetegi, "A series solution for the single-mode synthesis problem based on the coupled-mode theory," *IEEE Transactions on Microwave Theory and Techniques*, vol. 56, no. 2, pp. 457-466, Feb 2008.

[14] Y. Qian, V. Radisic, and T. Itoh, "Simulation and experiment of photonic band-gap structures for microstrip circuits," *Proceedings of the 1997 Asia-Pacific Microwave Conference*, Hong Kong, Dec. 1997, pp. 585-588.

[15] T. Lopetegi, M. A. G. Laso, M. J. Erro, D. Benito, M. J. Garde, F. Falcone, and M. Sorolla, "Novel photonic bandgap microstrip structures using network topology," *Microwave and Optical Technology Letters*, vol. 25, no. 1, pp. 33-36, April. 2000.

[16] T. Lopetegi, M. A. G. Laso, R. Gonzalo, M. J. Erro, F. Falcone, D. Benito, M. J. Garde, P. de Maagt, and M. Sorolla, "Electromagnetic crystals in microstrip technology," *Optical Quantum Electron.*, vol. 34, no. 1-3, pp. 279-295, Jan.-Mar. 2002.

[17] T. Lopetegi, M. A. G. Laso, M. J. Erro, M. Sorolla, and M. Thumm, "Analysis and design of periodic structures for microstrip lines by using the coupled-mode theory," *IEEE Microw. Wireless Compon. Lett.*, vol. 12, no. 11, pp. 441-443, Nov. 2002.

[18] I. Arnedo, J. D. Schwartz, M. A. G. Laso, T. Lopetegi, D. V. Plant, and J. Azaña, "Passive Microwave Planar Circuits for Arbitrary UWB Pulse Shaping," *IEEE Microw. Wireless Compon. Lett.*, vol. 18, no. 7, pp. 452-454, July 2008.

[19] G. H. Song and S. Y. Shin, "Design of corrugated waveguide filters by the Gel'fand-Levitan-Marchenko inverse-scattering method," *J. Opt. Soc. Amer. A*, vol. 2, no. 11, pp. 1905-1915, Nov. 1985.

[20] Moe Z. Win and Robert A. Scholtz, "Ultra-Wide Bandwidth Time-Hopping Spread-Spectrum Impulse Radio for Wireless Multiple-Access Communications," *IEEE Transactions on Communications*, vol. 48, no. 4, pp. 679-691, April 2000.

[21] D. M. Pozar, *Microwave Engineering*, Second Edition, Reading, MA: Addison-Wesley, 1998.